TURBULENT CHARACTERISTICS OF SHALLOW FLOW OVER ROUGH SURFACE WITH REGULARLY ARRAYED SPHERES

Sukarno
Department of Civil and Environmental Engineering,
Sam Ratulangi University, Indonesia
E-mail: sukarno091@yahoo.com

Abstract

Turbulent nature of near-bed flow field was investigated in an open channel over a rough-bed artificially arrayed with glass beads, where ratios of the glass diameter to flow depth are 0.3, 0.5 and 0.8. Detailed spatial measurements of streamwise and vertical velocity fluctuations were made using Particle Image Velocimetry (PIV) in a vertical plane along the completely rough bed surface. Results indicated significant degrees of spatially regular variation in the time-averaged velocities, in which the upflow generated over upper region of roughness top is about 8% of the cross sectional average velocity, much stronger than the downflow. In addition, Reynolds shear stress and turbulent intensity showed minimum values at the ridge of roughness elements and maximum ones at the trough. These organized flow structure were suggested to be due to the vortex shedding brought about by the roughness elements.

Keywords: turbulent characteristics, bed-flow, streamwise, velocity, roughness

INTRODUCTION

Flow that is relatively shallow for the roughness of the surface over which it passes is typically found in gravel-bed streams in mountainous areas, flows over the ground surface or road surfaces, flows in steep channels and flows over revetments. Studies on flows over rough surfaces in the field of hydraulic engineering used to take place mainly in the form of applied research on drag and on resistance laws [Kanda T., Suzuki K. (1985), Kikkawa H. et al.(1988)], basic research on average flow characteristics and turbulence structures [Grass, A. J. (1971), Nezu I.(1977), Raupach, M. R. (1981), Raupach, M. R.et al..(1988)], and field investigations [Roy, A. G. et al. (2004)] from the viewpoint of flood control and water utilization. In recent years, studies from the viewpoint of river environment restoration have also been conducted [Nikora, V. I. et al. (2002)].

Fewer studies have been conducted on direct numerical simulation of turbulent flow over a rough surface than on a smooth surface because of the extreme difficulty in setting boundary conditions although there have been some creative approaches to boundary condition setting [Nakayama A. And Sakio K. (2003)]. Details of flows near rough boundaries remain largely unknown.

Shallow flow, which is the subject of this study, has been studied by Nakagawa et al. and others [Nakagawa, H., .et al.. (1989)]. It has been observed that near a river bed surface arrayed with spherical roughness elements, mean velocity distribution and turbulence intensity tend to become uniform, and the Reynolds stress falls locally. It has been pointed out that these characteristics are dependent on separation vortices and shed vortices from roughness elements.

Using the results of laser velocimeter measurement, Nezu et al. (1989) evaluated the influence of large-diameter roughness elements on water surface fluctuations, turbulence structures and turbulent energy budget of flow over a rough surface.

Nikora et al. (2002), using an ultrasonic velocimeter, conducted measurements of flow over an open channel bed arrayed with spherical roughness elements covered with periphytic algae and investigated the interaction between the biofilm and the near-bed flow. As a result, they found that biofilm increases roughness by 16 to 21% and reduces mean flow velocity, Reynolds stress, turbulence intensity and the vertical turbulent flux of turbulence energy. They also pointed out that biofilm reduces total spectrum

energy without significantly affecting the spectral distribution of velocity fluctuations over the roughness elements, and that sweep phenomena in coherent vortex structures are important for supplying nutrients to periphytic algae.

Cooper et al. (2004) reported that in a flow over a homogeneous gravel bed surface, spatial fluctuations in the time-averaged velocity of near-surface flow in the horizontal plane were as large as 21% of the space-averaged velocity in the same horizontal plane, and pointed out that such fluctuations increase with water depth.

Thus, flow near a gravel bed is very important for the habitats of benthos including periphytic algae. Many of the previous studies, however, were experimental studies based on point measurement made with hot-wire flow meters and laser Doppler velocimeters and did not fully investigate the spatial fluctuation characteristics of flow.

In this study, flow over a bed arrayed with spherical roughness elements, which is a basic model of flow over a gravel bed, was measured by particle image velocimetry (PIV). The measurement revealed that in the case of shallow flow over a rough surface, there are stable, highly regular upflows and downflows near the roughness elements. This paper investigates flow near a rough surface and the influence of the vertically averaged velocity of such flow on main flow velocity and the turbulence characteristics of such flow.

TEST APPARATUS AND METHODS

The flume used in the test is a variable-slope, re-circulating straight flume that is 10 m long, 40 cm wide and 20 cm high. The measurement zone is made entirely of acrylic plastic so that laser beam can be radiated from the sidewalls. Table 1 shows the test conditions. As shown in Figure 1, a right-handed coordinate system is used for the measurement zone. The direction of flow is the x-axis, the transverse direction is the y-axis, and the vertical direction is the z-axis; and the corresponding mean velocity components and fluctuating velocity components are U, V and W and u', v' and w', respectively.

On the flume bed in a 3-m-long section starting from a distance of 2 m from the upstream end of the flume, glass balls 15 mm in diameter were arranged in two layers in a close-packed manner. As shown in Figure 2, two cases of rough surface configuration were considered: BC1 (Boundary Condition 1, in which the ridge lines and trough lines formed by the glass balls are parallel with the direction of flow and BC2 (Boundary Condition 2), in which the same lines are perpendicular to the direction of flow. Both BC1 and BC2 were considered in Case 1, and only BC1 was considered in Case 2 and Case 3. As is clearly shown in Table 1, the roughness Reynolds number exceeds 70 in all cases, indicating a perfectly rough surface.

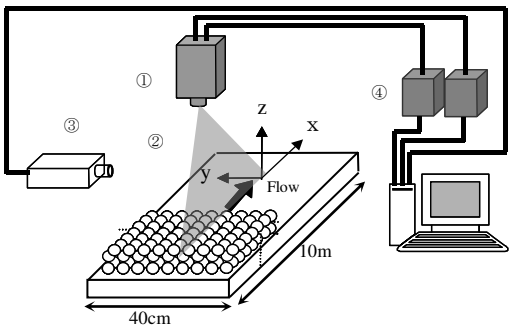

①Double- pulsed LASER Illumination System
②Lcaser sheet
③CCD-Camera Kodak Mega plus ES1.0
④YAG-Laser Main unit
⑤P.C.with Visiflow-software(Timing control & Analyze)

Fig 1. Experimental apparatus

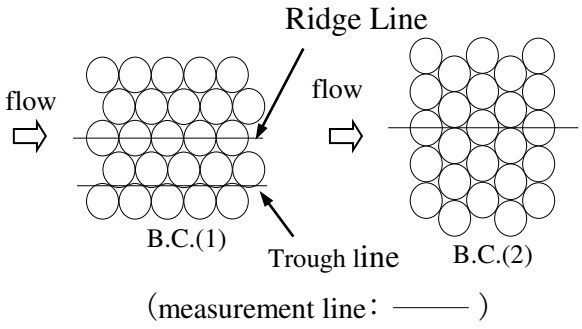

Fig 2. Boundary conditions (plan view)

Table 1. Experimental conditions

	Case1	Case2	Case3
Flow velocity U_m(cm/s)	35.0	26.3	35.0
Flow depth H(cm)	5.0	3.0	1.88
Channel slope I_o	1/500	1/500	1/178
Aspect ratio B/H	8	13.3	21.2
Froude num. $U_m/(gH)^{1/2}$	0.5	0.5	0.8
Reynolds num. U_mH/ν	17500	7800	6500
Rughness Reynolds num. u_*D/ν	470	363	483
Relative roughness D/H	0.3	0.5	0.8

Measurements were taken at a location 2.5 m from the end of the glass ball rough surface. In the flume, water was allowed to flow at a predetermined rate and the weir at the downstream end was adjusted to create uniform flow.

Flow velocity was measured by particle image velocimetry, which is a representative non-contact image processing method. Figure 1 illustrates the measurement system.

An air-cooled double-pulse YAG laser (25 mJ) was used as the light source. The laser light sheet thickness was 1 mm, and the pulse interval was 500 μs. For measurement in the xz plane, laser was radiated downward vertically onto the flume bed. For measurement in the xy plane, laser was radiated horizontally through the sidewall. Visualized images acquired by synchronized use of laser and a CCD camera were recorded on the hard disk of a personal computer in the form of 15-fps (frame per second) 960×1,018-pixel, monochromatic video data and were processed by PIV. Lenses with focal lengths of 50 mm and 200 mm were used. The former was used for a shooting range of 50 mm or more, and the latter was used for a shooting range of 15 mm or less to acquire detailed images of near-gravel regions. The minimum pixel size was 0.06 for the 50 mm lens and 0.016 mm for the 200 mm lens. The velocity sampling frequency was 15 Hz. The number of images per measurement plane was 1,000, and the measurement time per plane was 66.7 sec. Nylon particles with a diameter of 30 μm and a specific gravity of 1.02 were used as tracers.

MEAN VELOCITY CHARACTERISTICS

Figure 3 to Figure 14 show the spatial distribution characteristics of the main flow velocity U in the vertical plane obtained by PIV and the vertical velocity component W. The origin of the vertical coordinate axis z was defined at the top of the glass ball as done by Nakagawa et al.

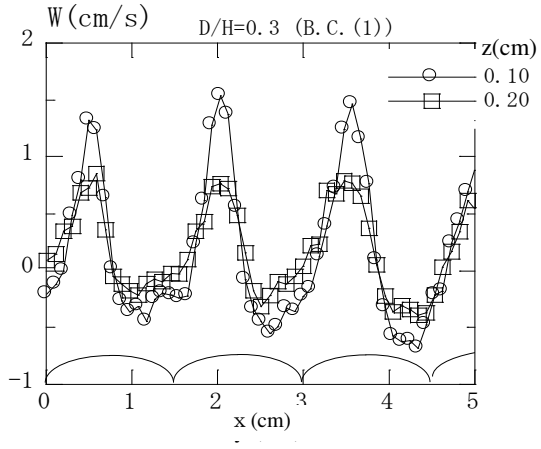

Fig 3. Longitudinal distribution of secondary flow velocity W (Case1-Ridge Line)

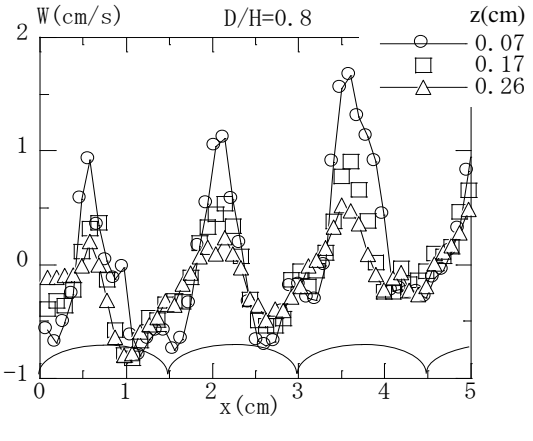

Fig 4. Longitudinal distribution of secondary flow velocity W (Case3 Ridge Line)

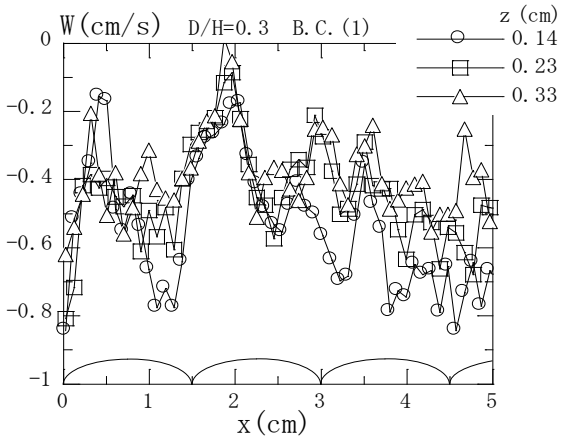

Fig 5. Longitudinal distribution of secondary flow velocity W (Case1-Trough Line)

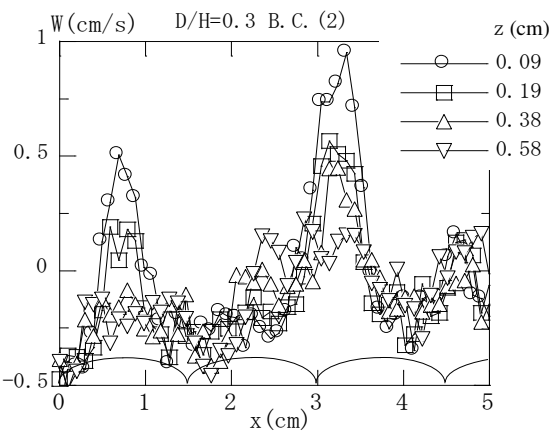

Fig 6. Longitudinal distribution of secondary flow velocity W (Case1)

Figure 3 and Figure 4 show changes in the flow direction in the vertical component W over the ridge line under the bed boundary condition BC1 in Case 1 (relative roughness: 0.3) and Case 3 (relative roughness: 0.8), respectively. As shown, in both cases, there are upflows a little upstream from the tops of the glass balls and there are downflows just downstream from the tops of the glass balls, and these patterns are highly regular. The maximum value of the upflow velocity is about 1.5 cm/s, indicating that upflow velocity tends to be high even in relatively small regions, while downflow velocity tends to be low even in relatively larger regions.

Figure 5 shows changes in the flow direction in the vertical component W over the trough line under the boundary condition BC1 in Case 1 (relative roughness: 0.3). The vertical component W over the trough line does not show any clear regularity as in the case of changes over the ridge line, and on the whole the downflows are relatively weak.

Figure 6 shows changes in the flow direction in the vertical component W over the ridge line under the boundary condition BC2 in Case 1 (relative roughness: 0.3). The vertical component W shows regularity correspond-ding to the cyclic length 2.73D of the bed. As in the BC1 cases shown in Figure 3 and Figure 4, upflows occur just upstream from the tops of the glass balls, and downflows occur in larger regions downstream from the tops of the glass balls.

These upflows, which are close to the bed but are stable and highly regular, indicate a close relationship between local pressure fields near the glass balls and separation vortices.

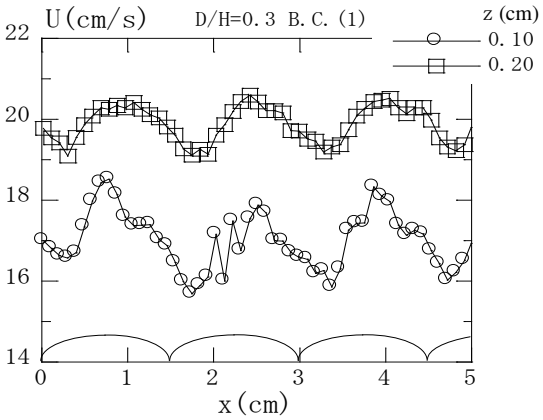

Fig 7. Longitudinal distribution of main flow velocity (Case1-Ridge Line)

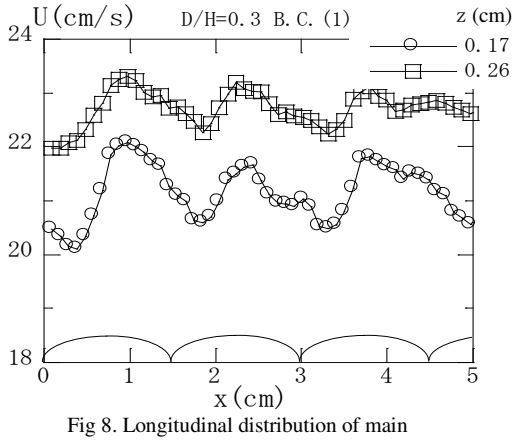

Fig 8. Longitudinal distribution of main flow velocity (Case3 Ridge Line)

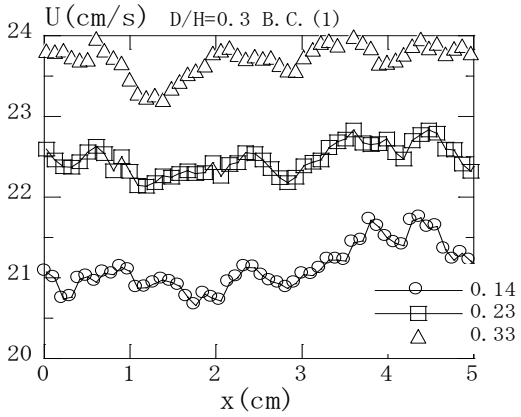

Fig 9. Longitudinal distribution of main flow velocity (Case1-Trough Line)

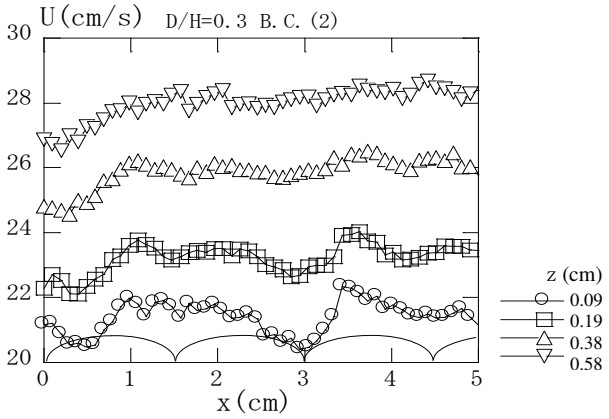

Fig 10. Longitudinal distribution of main flow velocity (Case1)

Figure 7 and Figure 8 show changes in the flow direction in the main flow velocity U over the ridge line under the boundary condition BC1 in Case 1 (relative roughness: 0.3) and Case 3 (relative roughness: 0.8), respectively. Like the vertical velocity component W, the main flow velocity shows highly regular changes in the flow direction and shows maximum values just upstream from the tops of the glass balls, indicating that their locations are close to the locations of the upflows. The minimum values of main flow velocity occur a little upstream from the locations of the upflow maximum values, indicating considerable differences from flow over a bed with longitudinal sand ridges [Ohmoto, T. & Hayashi, S. (2003)] as low velocities are generally shown in the downflow regions.

Figure 9 shows changes in the flow direction in the main flow velocity U over the trough line under the boundary condition BC1 in Case 1 (relative roughness: 0.3). Like the vertical velocity component W, the main flow velocity over the trough line does not show any clear regularity and shows only small changes in the direction of flow.

Figure 10 shows changes in the flow direction in the main flow velocity U over the ridge line under the bed boundary condition BC2 in Case 1 (relative roughness: 0.3). As in the BC1 cases shown in Figure 7 and Figure 8, the main flow velocity U clearly shows regular wave patterns and also shows maximum values near the tops of the glass balls and low velocities in the downflow regions.

Figure 11 and Figure 12 show in detail changes in the flow direction in the main flow velocity U and the vertical velocity component W occurring over the diameter of a single particle, measured with a high-resolution PIV system using a 200 mm lens. As shown, the vertical velocity component W is an upflow in the region upstream of the tops of the glass balls and a weak downflow in the region downstream from the tops of the glass balls. The maximum value of the upflow velocity is about 8% of the cross-sectionally averaged velocity. This value is large because the velocity of secondary flow over a bed with longitudinal sand ridges or in a channel with a rectangular cross section is usually several percent of the cross-sectionally averaged flow velocity. It is also shown that the maximum values occur about D/8 upstream from the tops of the glass balls.

The changes in the flow direction shown by the main flow velocity are similar to those shown by the vertical velocity component W. The maximum values of the main flow velocity are located about D/8 upstream from the tops of the glass balls. At the height about 1 mm above the tops of the glass balls, the amount of change in main flow velocity in the flow direction is about 10% of the cross-sectionally averaged velocity.

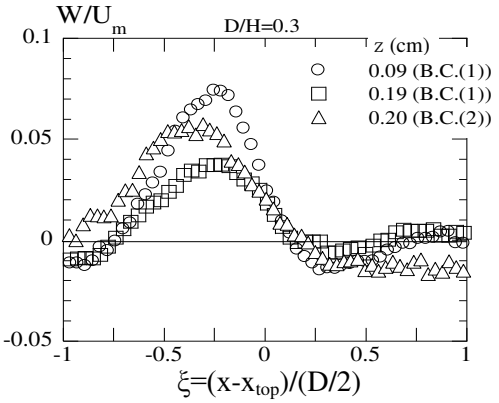

Fig 11. Longitudinal distribution of secondary flow velocity W

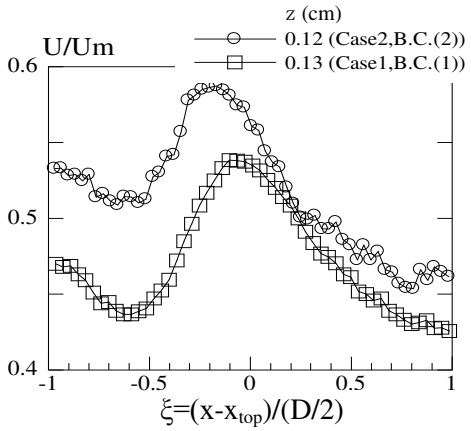

Fig 12. Longitudinal distribution of main flow velocity

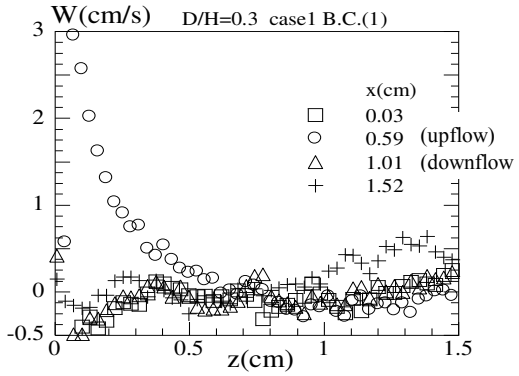

Fig 13.Vertical distribution of secondary flow velocity (Case 1)

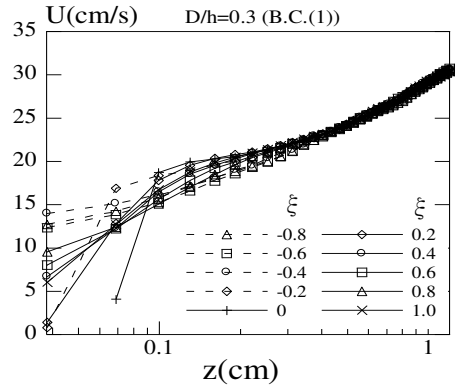

Fig 14. Vertical distribution of main flow Velocity (Case 1)

Figure 13 and Figure 14 show changes in the vertical direction in the vertical velocity component W and the main flow velocity U, respectively, over the ridge line under the bed boundary condition BC1 in Case 1 (relative roughness: 0.3). In the case of x=0.59cm, in which the maximum value occurred in the flow direction, the upflow velocity tends to reach the maximum value near the glass ball wall and then decrease uniformly in the vertical direction. Similarly, the downflow velocity tends to reach the maximum value near the wall and decrease uniformly. Both upflow and downflow velocities are nearly zero in the layers D/3 (z=5mm) or more above the tops of the glass balls. The main flow velocity U near the wall is higher in the upflow region than in the downflow region, and the difference between

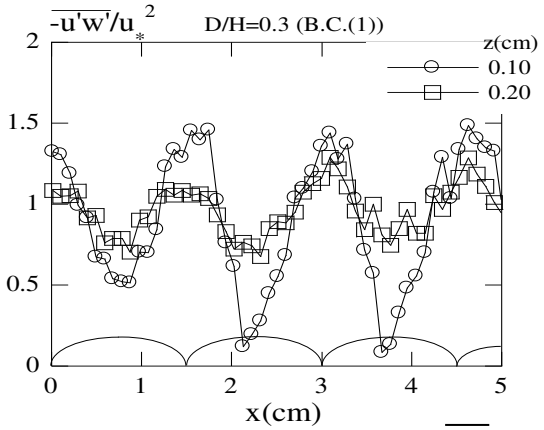

Fig 15. Longitudinal distribution of –u'w' (Case1, Ridge Line)

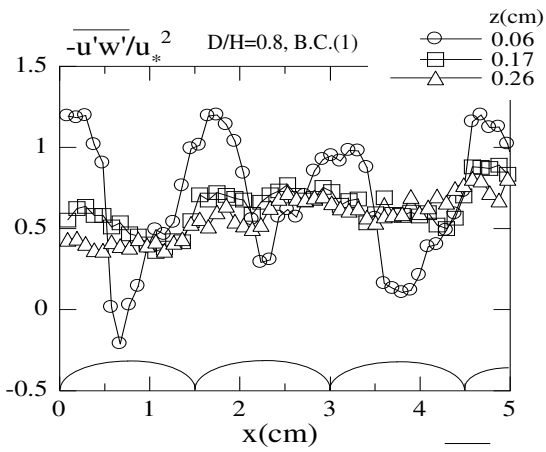

Fig 16. Longitudinal distribution of –u'w' (Case3, Ridge Line)

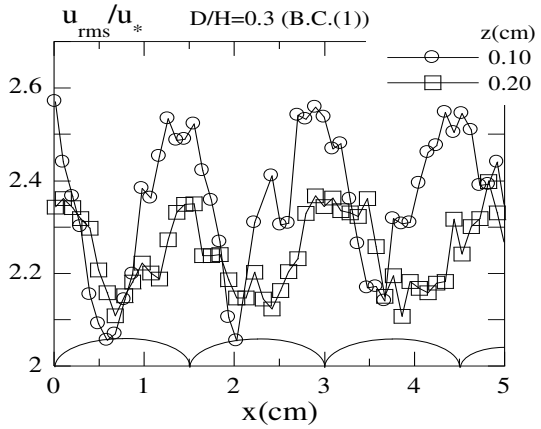

Fig 17. Longitudinal distribution of urms/u*
(Case1, Ridge Line)

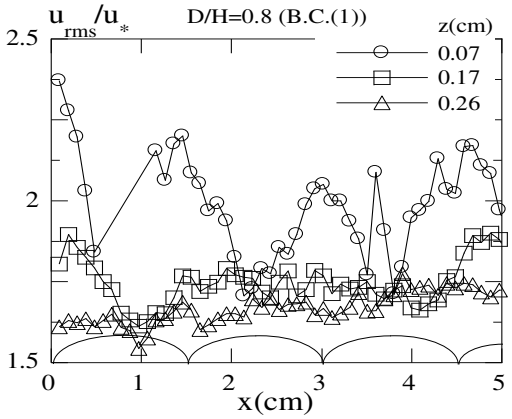

Fig 18. Longitudinal distribution of u_{rms}/u_*
(Case1)

the velocities in these regions decreases in the vertical upward direction. Like the vertical velocity component W, the main flow velocity also is almost zero in the layers D/3 (z=5mm) or more from the tops of the glass balls. In the acceleration zone, the main flow velocity tends to be uniform in the vertical direction, while in the deceleration zone it tends to change considerably in the near-wall region.

TURBULENCE CHARACTERISTICS

Figure 15 to Figure 18 show changes in the flow direction in the Reynolds shear stress and the turbulence intensity u_{rms}/u_* over the ridge line under the bed boundary condition BC1.

As shown in Figure 15 and Figure 16, the Reynolds shear stress over the ridge line changes considerably in the near-wall region, and reaches the minimum values over the tops of the glass balls and reaches the maximum values over the troughs. The distribution pattern is highly regular and is close to a sine wave with a wavelength equal to the particle diameter D and a wave height of u_*^2.

Like the Reynolds shear stress, the turbulence intensity u_{rms}/u_* varies considerably in the flow direction, and reaches the minimum values over the tops of the glass balls and the maximum values over the troughs. The distribution pattern is highly regular and is close to a sine wave with a wavelength equal to the particle diameter D and a wave height of $0.5u_*$.

Unlike the results observed over a bed with longitudinal sand ridges [Ohmoto, T. & Hayashi, S. (2003)], the Reynolds stress and the turbulence intensity are small near the upflow regions

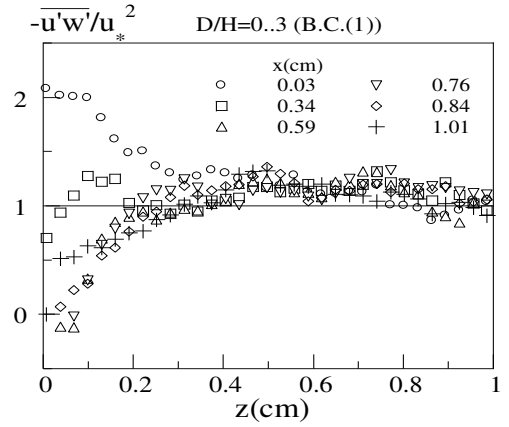

Fig 19.Vertical distribution of $-\overline{u'w'}/u_*^2$
(Case1, Ridge Line)

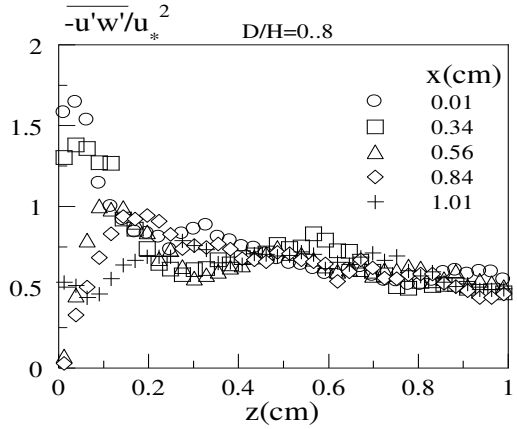

Fig 20.Vertical distribution of $-\overline{u'w'}/u_*^2$
(Case3, Ridge Line)

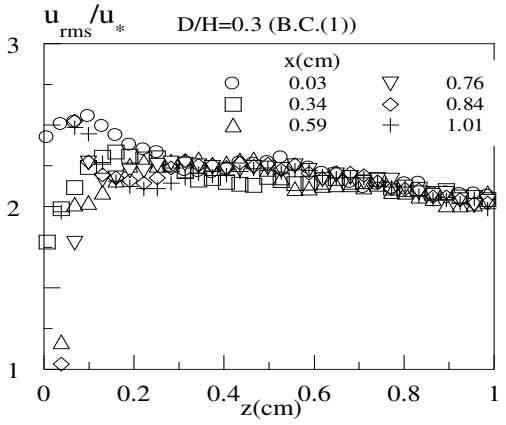

Fig 21.Vertical distribution of u_{rms}/u_* (Case1, Ridge Line)

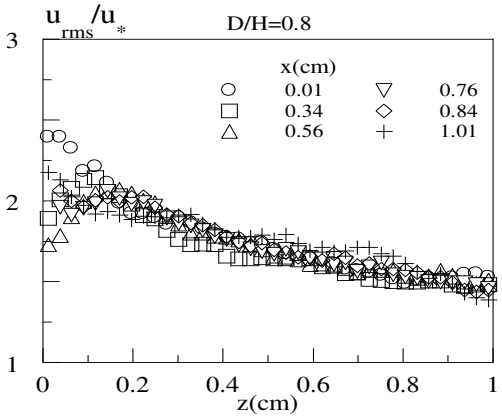

Fig 22. Vertical distribution of u_{rms}/u_* (Case1)

As can be seen from Figure 12, near the rough surface, the region from the top of the glass ball to D/4 upstream from the top of the glass ball is a high acceleration zone, and the region downstream of that region is a deceleration zone, so the influence of the pressure fields created by the roughness was strong.

Figure 19 to Figure 22 show changes in the vertical direction in the Reynolds stress and the turbulence intensity over the ridge line under the bed boundary condition BC1. As shown in Figure 19 and Figure 20, in the flow direction, the Reynolds shear stress is large over the troughs and small over the ridges. In the vertical direction, it is attenuated over the troughs and increases over the ridges as the distance from the roughness elements increases. At z=5 mm or so, there is no significant difference between the troughs and the ridges.

Figure 19 and Figure 21 indicate that the Reynolds shear stress and the turbulence intensity do not show significant differences between the flow distance of x=0.59 cm, at which the upflow showed the maximum value over the ridge line in Case 1, and x=1.01 cm, at which the downflow showed the maximum value. This can also be seen from Figure 20 and Figure 21.

Non-uniformity in the Reynolds shear stress and the turbulence intensity near the roughness elements is particularly noticeable near the roughness elements when roughly z<0.5cm (=D/3). This agrees with the results reported by Nezu et al. (1998).

CONCLUSION

In this study, flow over a bed arrayed with spherical roughness elements, which is a basic model of flow over a gravel bed, was measured by particle image velocimetry (PIV),which enables planar measurement. In the case of flow in the roughness sublayer, which was defined by Raupach et al. (1988), uniformity of the average flow and turbulence is greatly affected by roughness of the bed surface. It has been found that under the strong influence of roughness elements, flow in the roughness sublayer has the following characteristics:

1) At the relative roughness (relative to water depth) of 0.3, 0.5 or 0.8, the existence of stable and highly regular upflows and downflows was observed near the roughness elements. The maximum velocity of upflows was about 8% of the cross-sectionally averaged velocity, and its location was D/8 upstream from the tops of the glass balls.
2) Near the rough bed surface, the main flow velocity also showed a highly regular wavy pattern along the spherical roughness elements. Over the ridge line, there was a high-acceleration zone just upstream from the top of each roughness element and a deceleration zone downstream from the top of each roughness element. Velocity fluctuations were as much as about 10% of the cross-sectionally averaged velocity. In the vertical direction, flow velocity in acceleration zones showed a tendency

toward uniformity, and velocity in deceleration zones tended to decrease sharply near the walls.

3) Over the ridge line, the Reynolds shear stress and the turbulence intensity urms/u* fluctuated considerably in the flow direction. The minimum values were reached over the tops of the roughness elements, and the maximum values were reached over the troughs. The Reynolds shear stress and the turbulence intensity showed sine-wave-like, highly regular waveforms with a wavelength equal to the particle diameter D.

REFERENCES

Kanda T.,Suzuki K.(1985) Characteristics of Resistance to Shallow Water Flows over Bed Roughened with Spheres, Proc. JSCE, No. 357, pp. 65-74.(in Japanese)

Kikkawa H, Uematsu R.,Jyo M. And Sekine M.(1988) An Experimental Study on Velocity Profiles over the Bed Roughened with Spheres or Hemispheres and Fluid Forces exerted on them, Proc. JSCE, No. 399, pp. 47-54. (in Japanese)

Grass, A.J. (1971) Structural features of turbulent flow over smooth and rough boundaries, J. Fluid Mech., Vol.50, part2, pp.233-255.

Nezu Iehisa(1977) Turbulence Intensities in Open Channel Flows, Proc.JSCE, No.261, pp. 67-76. (in Japanese)

Raupach,M.R. (1981) Conditional statistics of Reynolds stress in rough-wall and smooth-wall turbulent boundary layers, J. Fluid Mech., Vol.450, pp.317-341.

Raupach, M.R.,Thom,A.S. and Edwards,L.A. (1988) A wind tunnel study of turbulent flow close to regularly arrayed rough surface, Boundary-Layer Meteorol.,18, pp.373-397.

Roy,A.G., Buffin-Belanger,T., Lamarre,H. and Kirkbride, A.D. (2004) Size, shape and dynamics of large-scale turbulent flow structures in a gravel-bed river, J. Fluid Mech., Vol.500, pp.1-27.

Nikora,V.I., Goring,D.G., and Biggs, J.F. (2002) Some observation of the effects of micro-organism growing on the bed of an open channel on the turbulence properties, J. Fluid Mech., Vol.450, pp.317-341.2

Nakayama A. And Sakio K.(2003) Direct Numerical Simulation of Turbulent Flow over Complex Wavy Rough Surface, Journal of Applied Mechanics, JSCE, Vol.6, pp839-846. (in Japanese)

Nakagawa,H.,Tsugimoto,T.and Shimiz,Y. (1989) Turbulent flow with small relative submergence, Proc. Int. Workshop on Fluvial of Mountain Regions, I.A.H.R, Trent, Italy, pp.A19-A30.

Nezu I.,Nakayama T. And Fujita M.(1998) Turbulence and Free-Surface Fluctuations in Open Channel Flows iver Macro-Roughness, Journal of Applied Mechanics, JSCE, Vol.1, pp709-718. (in Japanese)

Cooper J.R. and Tait. S. J. (2004) The spatial nature of the near-bed flow field over a naturally-formed gravel-bed, 5th International Symposium on Ecohydraulics,Madrid, Spain,Vol.1,pp.287-292.

Ohmoto, T. & Hayashi, S. (2003) Study on Generation Mechanism of Secondary Currents in Open-Channel Flow by Direct Numerical Simulation, Journal of Hydroscience and Hydraulic Engineering, Vol. 21, No. 1, pp.11-21, JSCE,